Single crystal EPR studies of Mn(II) doped into zinc ammonium phosphate hexahydrate ($ZnNH_4PO_4 \cdot 6H_2O$): A case of interstitial site for bio-mineral analogue

H ANANDALAKSHMI, K VELAVAN, I SOUGANDI, R VENKATESAN and P SAMBASIVA RAO

Department of Chemistry, Pondicherry University, Pondicherry 605 014, India
Email: psr52in@yahoo.co.in; psr52in@sify.com

Abstract. Single crystal EPR studies of Mn(II)-doped zinc ammonium phosphate hexahydrate ($ZnNH_4PO_4 \cdot 6H_2O$) have been reinvestigated at room temperature. Single crystal rotations along the three orthogonal axes indicate that the spin Hamiltonian parameters for the interstitial site are: $g_{xx} = 1.966$, $g_{yy} = 1.972$, $g_{zz} = 1.976$; $D_{xx} = -12.28$ mT, $D_{yy} = -2.09$ mT and $D_{zz} = 14.37$ mT; $A_{xx} = 9.06$ mT, $A_{yy} = 9.06$ mT and $A_{zz} = 11.09$ mT; $a = -0.11$ mT. These parameters differ considerably from the previous report of Chand and Agarwal and indicate the orthorhombic nature of the paramagnetic impurity. The impurity is found to enter the lattice interstitially, in contrast to earlier prediction of substitutional position. The percentage covalency of the Mn–O bond has been estimated.

Keywords. EPR; interstitial; distortion; spin Hamiltonian; invariant.

PACS Nos 61.72.Hh; 76.30.Fc

1. Introduction

EPR of Mn(II) has been widely studied in a variety of crystals [1–5], with the main emphasis of determining site symmetry and orientations, study of phase transitions and the magnetic properties of the materials. In addition, the effect of charge compensation is also studied in Mn(II)-doped single crystals. The impurity ions, such as transition metal ions, are responsible for modification of many physical properties and play a major role in devices like wave-guides, holography and electro-optical devices [6,7]. The Mn(II) ion has been used as a probe in large varieties of host lattices because it shows no Jahn–Teller effect and hence its EPR spectra reflect the true point symmetry. In the case of Mn(II), the zero-field splitting is highly sensitive to local field geometry and hence, the nature of site symmetry can be elucidated very easily with EPR studies. EPR study of Mn(II) in different types of host lattices

have been done; a few examples are discussed below. The EPR study of Mn(II)-doped cadmium maleate dihydrate indicates that Mn(II) is found to enter the host lattice interstitially and exhibit distorted octahedral symmetry [8]. In cis-catena-μ-sulphato-aquotris(imidazole) cadmium(II), the paramagnetic ion enters substitutionally into the host lattice giving rise to two magnetically inequivalent sites [9]. Single crystal EPR study of Mn(II)-doped magnesium bis(hydrogen maleate) hexahydrate confirms that the impurity ion not only occupies the magnesium site in a substitutional way but also in an interstitial site [10]. Thus the ion can enter the lattice in a substitutional way or interstitial position or both. Literature survey reveals that in a paramagnetic host lattice such as nickel bis(hydrogenmaleate) hexahydrate (NHMH), Mn(II) ion enters the lattice substitutionally in the place of Ni(II) with orthorhombic distortion [11].

Paramagnetic ions like Cu(II) [12] and VO(II) [13] are studied in zinc ammonium phosphate hexahydrate ($ZnNH_4PO_4·6H_2O$) abbreviated as ZAPH. EPR studies of Cu(II) in ZAPH reported over a wide range of temperatures indicate that the co-ordination polyhedron around the host Zn(II) ion corresponds to a tetragonally compressed octahedron of oxygen atoms of water. The g and A tensor direction cosines match fairly well with one of the Zn–O directions, confirming that Cu(II) enters the lattice in place of Zn(II). In the case of VO(II)-doped ZAPH, the paramagnetic impurity substitutes for the host divalent ion and gets associated with one oxygen to form a vanadyl bond (V=O) along a favourable metal–water bond within a given octahedron with different preference. There are two distinct favourable directions for a V=O bond which result in two distinct vanadyl complexes. Also, EPR studies of Mn(II) in ZAPH has indicated that the impurity has entered the lattice substitutionally and exhibits two magnetically inequivalent sites, as expected from the crystal structure of the host lattice [13]. However, during the single crystal work of Cu(II)/ZAPH [12], the manganese impurity has entered the lattice along with Cu(II) and exhibits only one site for Mn(II) during crystal rotations. Hence, in order to understand the nature of the location of Mn(II) in ZAPH, single crystal work has been undertaken. The results are interesting in the sense that the paramagnetic impurity has entered the lattice interstitially, in contrast to the previous observation of Chand and Agarwal [13]. The spin Hamiltonian parameters are also different. Also, the relative signs of the zero-field parameters have been ascertained and the percentage covalency of the metal–ligand bond has been estimated. These results are presented in this communication with a detailed single crystal work.

2. Experimental technique

Single crystals of $ZnNH_4PO_4·6H_2O$ (ZAPH) are grown by the slow evaporation of equimolar aqueous solutions of ammonium dihydrogen phosphate (11.60 g) and zinc sulphate (28.75 g). To this, 0.1% of the paramagnetic impurity has been added in the form of manganous sulphate. Colourless transparent single crystals are obtained within 15 days. Crystals of optimum size are selected for EPR studies. The EPR spectra are recorded using a JEOL JES-TE100 ESR spectrometer operating at X-band frequencies and having a 100 kHz modulation to obtain first derivative EPR signal. The single crystal is mounted on a goniometer and spectra are recorded

for every 10° rotations. In order to extract the magnetic parameters, single crystal rotations have been done in the three mutually orthogonal planes.

3. Crystal structure

ZAPH is analogous to the biomineral, struvite ($MgNH_4PO_4 \cdot 6H_2O$), which belongs to orthorhombic system with unit cell dimensions $a = 0.6941(2)$, $b = 0.6137(2)$ and $c = 1.1199(4)$ nm. The space group is $Pmn2_1$ and there are two molecules per unit cell [14]. The structure consists of tetrahedral PO_4^{3-}, octahedral $Zn(H_2O)_6$ and NH_4 groups held together by hydrogen bonding. The metal atom is surrounded by six water molecules in a much distorted octahedral configuration with M–O distances ranging from 0.2046 to 0.2107 nm. Each oxygen atom is bonded to four other atoms, one phosphorus and three hydrogen atoms. The bonding atoms are at the corners of a distorted tetrahedron, the average oxygen–hydrogen bondlength being 0.193 nm compared to 0.1537 nm obtained for the average phosphorus–oxygen distance. The direction cosines of the three Zn–O directions in ZAPH lattice are given in table 1.

4. Results and discussion

Mn(II), being a d^5 ion, is very sensitive to distortions from perfect octahedral or tetrahedral symmetries. Hence, a number of EPR studies have been undertaken with Mn(II) as the probe to study distortions, phase transitions etc [15–17]. The six spin states labeled as $|\pm 5/2\rangle, |\pm 3/2\rangle$ and $|\pm 1/2\rangle$ are the three Kramers' doublets separated by $4D$ and $2D$ respectively, in the absence of an external magnetic field. Here, D is zero-field splitting parameter. When an external magnetic field is applied, these spin states split further and one can observe five EPR transitions with selection rule $\Delta Ms = \pm 1$. Each of these five lines split further into a sextet, due to the nuclear spin of manganese ($I = 5/2$). Hence, one expects a 30-line pattern. However, in polycrystalline samples, only $|+1/2\rangle \leftrightarrow |-1/2\rangle$ transition is generally observed, since the other four transitions have large anisotropy [15]. If D is very small compared to hyperfine coupling constant (A), the 30 lines will be so closely packed that one could see only six lines. On the other hand, if D is very large, one would expect five bunches of resonance lines, each split into a sextet.

Table 1. Direction cosines of the three Zn–O directions in zinc ammonium phosphate hexahydrate host lattice and that of the distortion axis. The distortion axis does not match with any one of the Zn–O directions (see text).

Axes	a	b	c
Zn–O1	0.0000	−0.8902	0.4556
Zn–O3	−0.7314	0.3344	0.5944
Zn–O4	−0.7143	−0.3265	−0.6190
Distortion axis	−0.8477	0.3666	0.3834

A good single crystal of optimum size of Mn(II)/ZAPH is selected for crystal rotations. Typical EPR spectrum in *ac* plane of rotation is shown in figure 1. This EPR spectrum is characteristic of a system with $S = 5/2$ and $I = 5/2$. Generally, if the impurity enters the lattice in two different positions, one would expect a 30-line pattern along any one of the crystallographic axes and 60 lines at other orientations. However, only a maximum of 30 lines have been observed in any orientation indicating the presence of only one site for the impurity, even though the lattice contains two molecules per unit cell. Hence, single crystal rotations are performed about the three orthogonal planes *ab*, *bc* and *ac* respectively. Except a small change in the maximum spread, the isofrequency plots are identical in two planes and remain almost invariant in the third orthogonal plane. One such isofrequency plot of Mn(II)/ZAPH in the *ac* plane showing all the hyperfine lines is given in figure 2. The simpler form of the road map showing only the main five transitions, excluding nuclear hyperfine from manganese nucleus, is given in figure 3. The crystal rotation performed in the other plane namely *ab* plane, has shown that the lines are slightly variant. The corresponding isofrequency plot in *ab* plane, considering only fine structure terms, is given in figure 4. The spin Hamiltonian for a spin multiplet, due to second-order effects and other zero-field terms like a and F, is given by [15]

$$
\begin{aligned}
H = {} & \beta B g S + A_{zz} S_z I_z + A_{xx} S_x I_x + A_{xx} S_y I_y + D[S_z^2 - 1/3 S(S+1)] \\
& + E(S_x^2 - S_y^2) + (a/6)[S_\alpha^4 + S_\beta^4 + S_\gamma^4 - (1/5) S(S+1)(3S^2 + 3S - 1)] \\
& + (F/180)[35 S_z^4 - 30 S(S+1) S_z^2 + 25 S_z^2 - 6 S(S+1) + 3 S^2 (S+1)^2].
\end{aligned}
$$

Using perturbation theory, the energy levels have been evaluated from the above equation. From the power series expression [1,18], the terms involving the cubic field, retaining only the major terms, have been reported.
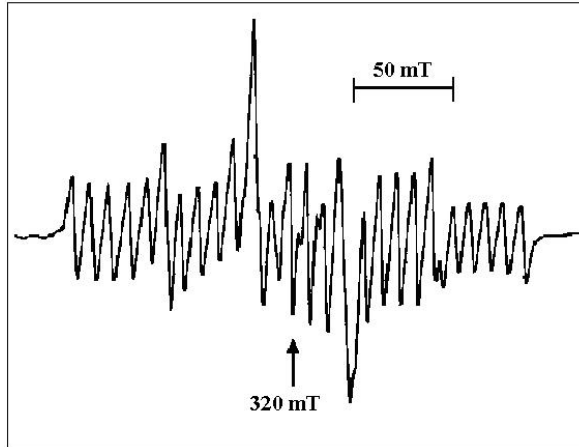

Figure 1. Typical EPR spectrum of Mn(II)/ZAPH at room temperature in *ac* plane of rotation at an arbitrary orientation of the crystal. Here one can notice the overlapping of the sixth hyperfine line of a set with the first hyperfine of the next set. $\nu = 9.07384$ GHz.
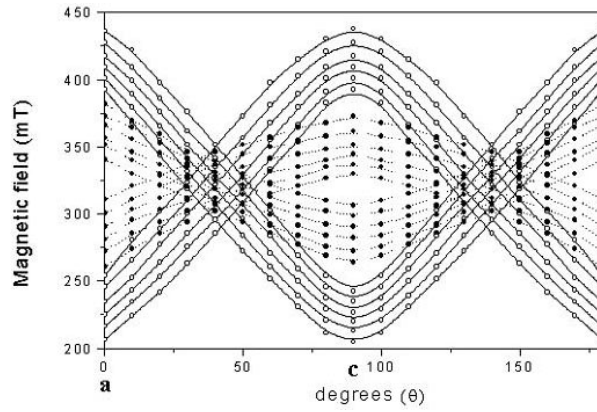
Figure 2. Isofrequency plot of Mn(II)/ZAPH in *ac* plane at room temperature. The transition $|+1/2\rangle$ to $|-1/2\rangle$, which is nearly invariant is not shown. $\nu = 9.07384$ GHz.
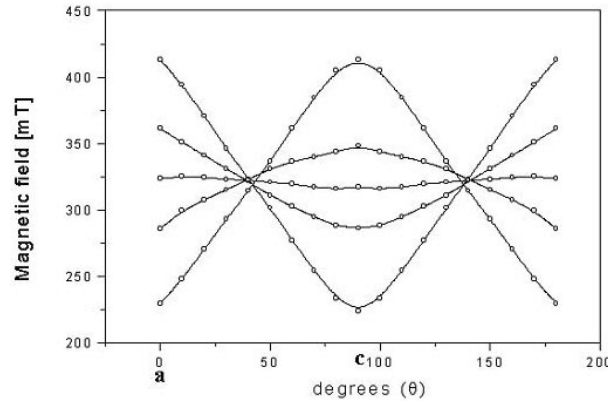

Figure 3. Isofrequency plot of Mn(II)/ZAPH in *ac* plane as shown in figure 2 except the hyperfine lines from manganese nucleus are not considered. Here, the transition $|+1/2\rangle$ to $|-1/2\rangle$ is also shown. $\nu = 9.07384$ GHz.

The major term, which determines the fine structure is D and is proportional to $(3\cos^2\theta - 1)$. The fine structure lines will also have a similar angular dependence, but slightly modified due to small contributions from a and D/E. If the magnetic field and the distortion axis are in the same direction, i.e., $\theta = 0$, the separation between $|+5/2\rangle \leftrightarrow |3/2\rangle$ and $|-5/2\rangle \leftrightarrow |-3/2\rangle$ transitions is maximum. The separation decreases as θ increases and the fine structure collapses at $\theta = 54°44'$, as $(3\cos^2\theta - 1) = 0$ at this angle. As θ increases further, a second maximum is obtained at $\theta = 90°$. The pattern will be repeated after $90°$ up to $180°$.

Using the three isofrequency plots and EPR-NMR program [19], the spin Hamiltonian parameters have been calculated and are given in table 2. Also given in the table are the results of previous study of Mn(II)/ZAPH [13], which differ considerably from our present values. From table 2, it is clear that the g matrix is close to

axially symmetric in nature and thus confirms the observation of roadmaps in all the three orthogonal planes. The direction cosines also confirm that the principal values of g matrix are not located along the major axis. The hyperfine matrix also behaves in a similar fashion and the direction cosines of A matched fairly well with those of g matrix, confirming the coincidence of g and A tensors. This also has been confirmed from the roadmap, since the maxima and minima occurred at the same angle for g and A values. However, the behaviour of D matrix is quite different. The three principal values are along the three directions, a common observation noticed in our previous cases of Ni(II)/HZDT [20]. The tensor has the asymmetry parameter, E, equal to 6.1 mT, slightly lower than the previous case of Mn(II) in ZPPH [21]. This non-zero value for E results in the invariance of hyperfine resonance lines in ab plane, as discussed earlier and justifies its inclusion in the spin Hamiltonian.

Direction cosines of the distortion axis are necessary to evaluate spin Hamiltonian parameters and to identify the location of the impurity. However, due to the presence of only one site, it was easy to calculate the direction of the distortion axis. In general, the distortion could be either tetragonal, i.e., along one of the axis of the Zn–O octahedron or trigonal, i.e., along $\langle 111 \rangle$ axis of the octahedron. A general procedure to identify the distortion axis has been discussed [10]. One has to obtain the zero field parameter from the powder spectrum to obtain the distortion axis. EPR spectrum of powder sample Mn(II)/ZAPH recorded at room temperature is given in figure 5. The unsymmetrical nature of the powder spectrum is a clear indication of the presence of E term in the spin Hamiltonian. The spin Hamiltonian parameters obtained from powder spectra are given in table 3, along with single crystal data of ours and a few related literature data. In the present case, the direction cosines of the distortion axis as derived above does not match well with any one of the Zn–O directions in the lattice (table 1). The angle between Zn–O3 direction and distortion axis is around 13°, which is rather high, indicating less chance of Mn(II) to enter into the lattice in the place of Zn. In a previous study in which Cu(II) is doped into this host lattice [14], the unique g-axis has
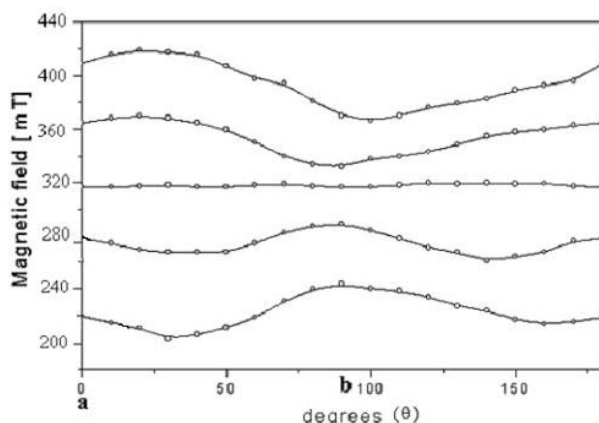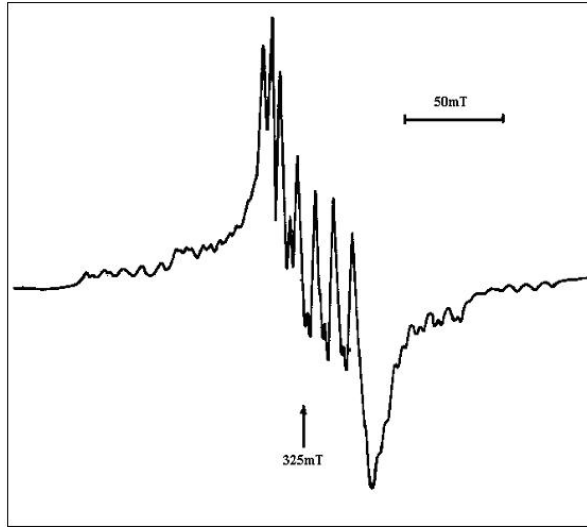

Figure 4. Isofrequency plot of Mn(II)/ZAPH in ab plane at room temperature. All the lines are almost invariant. $\nu = 9.11293$ GHz.

Table 2. Spin Hamiltonian parameter (g, A and D) matrices calculated from the isofrequency plots, using the program EPR-NMR [19].

			Eigenvalues	Direction cosines		
				a	b	c
g matrix						
1.973	0.004	−0.003	1.966	−0.4954	−0.0102	−0.8686
	1.973	−0.003	1.972	0.6059	−0.6999	−0.3476
		1.969	1.976	0.6044	0.7142	−0.3531
D matrix (mT)						
−2.09	0.00	0.00	−12.28	−0.0049	0.0000	−0.9999
	14.37	−0.13	−2.09	0.9999	0.0000	−0.0049
		−12.28	14.37	0.0000	1.0000	0.0000
A Matrix (mT)						
9.06	0.001	−0.0721	9.06	0.9994	0.0000	0.3347
	9.06	−0.0721	9.06	−0.0246	−0.7071	0.7067
		11.09	11.09	−0.0246	0.7071	0.7067

Figure 5. Powder EPR spectrum of Mn(II)/ZAPH at room temperature, indicating the orthorhombic nature of D (see text). $\nu = 9.40231$ GHz.

been found to be along Zn–O3 direction, the angle being less than 5°. It is also to be pointed out here that in the case of Cu(II), two magnetically inequivalent sites have been noticed, whereas it is not so in the present study.

In order to evaluate the relative signs and magnitudes of D and a, the following procedure is used. The separation between the extreme sets of hyperfine sextets, corresponding to the transitions $|+5/2\rangle \leftrightarrow |+3/2\rangle$ and $|-5/2\rangle \leftrightarrow |-3/2\rangle$ is

Table 3. Magnetic resonance data for Mn(II) (d^5, high-spin) in some related host lattices (D, E, A and a are in mT).

System	g_{xx}, g_{yy}, g_{zz}	A	D	E	a	Ref.
MMHH	1.995	9.6	33.44	–	0.40	[10]
NHMH	2.021	8.2				
	2.024	8.2	21.60	2.89	0.09	[11]
	2.024	8.2				
MHMH	1.997	8.8				
	2.013	8.8	31.20	3.47	0.12	[11]
	2.013	8.8				
$CoH_6CeMo_{12}O_{42.12}H_2O$	2.017	7.7				
	2.003	7.7	22.40	3.70	–	[12]
	2.003	8.2				
ZPPH	1.999	11.7	15.49			
	1.954	10.5	0.22	7.64	0.08	[21]
	1.952	10.4	−15.71			
ZAPH	2.002	9.2	53.52	8.67	–	[13]
	2.001	9.2	−35.41			
	2.001	9.3	−18.11			
ZAPH	1.966	9.1	−12.28			Present
Single crystal data	1.972	9.1	−2.09	6.1	−0.11	study
	1.976	11.1	14.37			
Powder data	2.041	9.1	23.21			

MMHH – magnesium maleate hexahydrate.
NHMH – nickel bis(hydrogen maleate) hexahydrate.
MHMH – magnesium bis(hydrogen maleate) hexahydrate.
ZPPH – zinc potassium phosphate hexahydrate.

$$B|+5/2\rangle \leftrightarrow |+3/2\rangle - B|-5/2\rangle \leftrightarrow |+3/2\rangle$$
$$= 4D(3\cos^2\theta - 1) + pa + 1/3F(35\cos^4\theta - 30\cos^2\theta + 3).$$

Any three orientations can be chosen to get the values of D, F and a. The values of D and a, which give best fit have been calculated and found to agree well with the values obtained from single crystal analysis. The value of F is found to be too small.

We have also calculated the percentage of covalency of the Mn–O bond from Matamura's plot [22,23]. The covalency of a bond between manganese and its ligands will certainly have an effect on the magnitude of the isotropic hyperfine coupling constant A. An approximate relationship for the covalency c of a bond between the atoms p and q and their electronegativities χ_p and χ_q is given by

$$c = [1 - 0.16(\chi_p - \chi_q) - 0.035(\chi_p - \chi_q)^2]/n.$$

Here, n is the number of ligands around Mn(II) ion. The percentage of covalency obtained is around 10.9, assuming $\chi_{Mn} = 1.4$ and $\chi_O = 3.5$ [24] and the value of

hyperfine splitting constant predicted from the graph agrees reasonably well with the observed value.

5. Conclusion

Thus, the spin Hamiltonian parameters (g, A, D and a) for Mn(II)/ZAPH have been obtained from single crystal rotation in the three orthogonal planes. The spin Hamiltonian parameters obtained in the present study are clearly different from those reported earlier by Chand and Agarwal. In addition, the location of the impurity, in our present case is interstitial, whereas it is substitutional in the other study. The deviation from axial symmetry is reflected more in D tensor than in g and A tensors. Powder EPR spectrum of Mn(II)/ZAPH confirms the presence of only one site in the host lattice and hence supports the single crystal data. The Mn–O bond seems to be almost ionic with only 13% covalency. The spin Hamiltonian parameters deviate from axial symmetry, confirming the orthorhombic nature of the paramagnetic impurity.

References

[1] D Pathinettam Padiyan, C Muthukrishnan and R Murugesan, *Spectrochim. Acta* (Part A) **58**, 509 (2002)
[2] T K Gundu and P T Manoharan, *Chem. Phys. Lett.* **264**, 338 (1997)
[3] B Wagner, S A Warda, M A Hitchman and D Reinen, *Inorg. Chem.* **35**, 3967 (1996)
[4] J Lech, A Slezak and R Hrabanski, *J. Phys. Chem. Solids* **52**, 685 (1991)
[5] F E Mabbs and D Collison, *Electron paramagnetic resonance of d-transition metal compounds* (Elsevier, Amsterdam, 1992)
[6] L Sree Ramachandra Prasad and S Subramanian, *J. Chem. Phys.* **83**, 1485 (1985)
[7] Wen-Chen Zheng, *Phys. Status Solidi* **B205**, 627 (1998)
[8] S N Rao, Y P Reddy and P S Rao, *Solid State Commun.* **82**, 419 (1992)
[9] R Murugesan, V S X Anthonisamy and S Subramanian, *Spectrochim. Acta* (Part A) **49**, 1801 (1993)
[10] Jesiamma Joseph and P Sambasiva Rao, *Spectrochim. Acta* **A52**, 607 (1996)
[11] R M Krishna, V P Seth, R S Bansal, I Chand, S K Gupta and J J Andre, *Spectrochim. Acta* (Part A) **54**, 517 (1998)

[12] E Poonghuzali, R Srinivasan, T M Rajendiran, R Venkatesan, P Sambasiva Rao, R V S S N Ravikumar, A V Chandrasekar, B J Reddy and Y P Reddy, *Phys. Scr.* 2002 (In press)

[13] P Chand and O P Agarwal, *Spectrochim. Acta* **A47**, 775 (1991)

[14] A Whitaker and J W Jeffery, *Acta Crystallogr.* **B26**, 1429 (1970)

[15] A Abragam and B Bleaney, *Electron paramagnetic resonance of transition metal ions* (Clarendon Press, Oxford, 1970)

[16] J R Pilbrow, *Transition ion electron paramagnetic resonance* (Clarendon Press, Oxford, UK, 1990)

[17] J A Weil, J R Bolton and J E Wertz, *Electron paramagnetic resonance: Elementary theory and practical applications* (John Wiley and Sons Inc., New York, 1994)

[18] E deL Kronig and C J Bouwkamp, *Physica* **6**, 290 (1939)

[19] EPR-NMR Program developed by F Clark, R S Dickson, D B Fulton, J Isoya, A Lent, D G McGavin, M J Mombourquette, R H D Nuttall, P S Rao, H Rinneberg, W C Tennant and J A Weil, University of Saskatchewan, Saskatoon, Canada (1996)

[20] K Velavan, T M Rajendiran, R Venkatesan and P Sambasiva Rao, *Solid State Commun.* **122**, 15 (2002)

[21] H Anandalakshmi, R Venkatesan and P Sambasiva Rao, *Spectrum. Acta (Part A)* (submitted)

[22] O Matamura, *J. Phys. Soc. Jpn.* **14**, 108 (1959)

[23] E Simanek and K A Muller, *J. Phys. Chem. Solids.* **31**, 1027 (1970)

[24] W Gordy and W J Orville-Thomas, *J. Chem. Phys.* **24**, 439 (1956)